Fission energy deposition in UO_2 through multi-scale/physics hierarchy modeling: From the first-principles and SRIM to molecular dynamics

Woong Kee Kim[a], Ji Hoon Shim[a,c,*] and Massoud Kaviany[a,b,*]

[a]*Division of Advanced Nuclear Engineering, Pohang University of Science and Technology, Pohang 37673, Korea*
[b]*Department of Mechanical Engineering, University of Michigan, Ann Arbor, Michigan 48109-2125, USA*
[c]*Department of Chemistry, Pohang University of Science and Technology, Pohang 37673, Korea*
[*]*Corresponding author: jhshim@postech.ac.kr, kaviany@umich.edu*

1. Introduction

Uranium dioxide is the most widely used nuclear fuel in commercial nuclear reactors. It has been used several decades in many reactor types due to its energy high melting temperature, radiation tolerance and high chemical stability. The fission process of uranium and its consecutive radiation events (delayed neutron emission, radio active decay, etc.) can be very disruptive of the fuel's atomic lattice and eventually will have significant ramifications on fuel integrity [1]. Study on radiation damage, such as non-equilibrium immediate damage process, evolution of damage and following recovery, has been of significance in radiation material science and nuclear engineering [2]. Energy of fission fragment is deposited via interactions with nuclei and electrons. In the atomistic scale of interactions, movement of FP in early stage is damped mainly by electrons through inelastic scattering process. Excited electrons (δ-ray) from inelastic scattering again transfer fission energy to the lattice as electron-phonon (e-p) coupling process. When FP lose the kinetic energy until order of keV, FP nuclei collide with adjacent nuclei in the material. Radiation damage on material has been mainly studied by two modeling approaches: cascade simulation using molecular dynamics (MD) and SRIM code [4] based on the binary collision approximation. Both approaches have made very successful results in the investigation of radiation damage, however, these also have each limitation due to its method to approximate. For cascade simulation, inelastic scattering from electron effect is neglected due to the limitation of empirical inter-atomic potentials in MD simulation [5,6], though it has provided very accurate descriptions on damage process. This MD approach is not valid when PKA has high kinetic energy that significant portion of energy is lost by electrons [6] as shown in right side of blue and red lines of lower right figure [7]. On the other hand, SRIM calculation which enables to calculated the interaction of ions with materials does not consider accurate description in atomic scale, such as defect recombination or the redistribution of the electronic energy to the lattice [8].

In this work, as an alternative approach which takes advantages from previous two approaches, interactions of PKA with both excited electrons and surrounding atoms are described using multi-physics/multi-scale approaches. In quantum-mechanical approach using the first principle calculation, e-p coupling in UO2 is described and related e-p coupling constants are calculated. From the calculated e-p coupling parameters, multiple heat deposition process including both electronic and lattice effects are simulated using classical molecular dynamics by two temperature model-MD (TTM-MD) frameworks.

2. Methods and Results

2.1 Two temperature model (TTM)

Two temperature model (TTM) provide the description on energy transfer between electronic and atomic subsystems. Energy exchange between the two subsystems are governed by the heat diffusion equation [9].

$$c_e(T_e)n_{e,c}\frac{\partial T_e}{\partial t} = \nabla(\kappa_e \nabla T_e) - g_{e-p}(T_e - T_p) + g_e T'_p, \quad (1)$$

where c, n, κ and T is heat capacity, number density, thermal conductivity and temperature, respectively. Subscript e and p represent electron and atomic subsystems. T_p' is local threshold temperature for movement of atoms as delta-ray dose term from fission energy deposition as the initial energy injection into the electronic sub-system [10]. $g_{e\text{-}p}$ indicate the electron-phonon coupling constant and g_e is the electron stopping constant. Electron is considered as continuum fields, in addition to conventional molecular dynamics model. Spatial and temporal continuum distributions of temperature (T_e) are solved numerically from initial electronic temperature profile. Two temperatures (T_e and T_P) are

eventually equilibrated as time goes on. Total energy of two subsystems are conserved

In original TTM, energy conservation equation or heat diffusion equation is also required for phonon as conjugate form of heat diffusion equation for electron. However, in TTM-MD frame works, heat diffusion equation for phonon is replaced with Langevin equation of motion in TTM-MD in below Eq. (2), which is also governing equation of movement of ion *i*.

$$\boldsymbol{F}_i = -\frac{\partial U}{\partial \boldsymbol{r}_i} - \gamma \boldsymbol{v}_i + \boldsymbol{F}'_{lang}(t), \quad (2)$$

where $\boldsymbol{F}_i$ is total force acting on atom *i*, *U* is conventional interatomic potential in MD simulation, γ is stopping coefficient including electron stopping (γ_s) and electron-phonon interactions($\gamma_{e\text{-}p}$). Above the electronic stopping critical velocity (v_0), $\gamma = \gamma_{e\text{-}p} + \gamma_e$, otherwise $\gamma = \gamma_e$. These coefficients are related with coupling constants, $g_{e\text{-}p}$ and g_e [6]. Total force acting on atom *i* is perturbed by friction term ($\gamma \boldsymbol{v}_i$) by both electron-phonon interaction and electronic stopping and bombardment with electrons expressed by stochastic force term ($\boldsymbol{F}'_{\text{lang}}$) determined by the local electronic temperature near atom *i* [7].

In TTM-MD frameworks, it requires input parameters, such as electron specific heat, electron density, electronic thermal conductivity and friction coefficient from electron-phonon coupling ($\gamma_{e\text{-}p}$) and from electronic stopping (γ_e). $\gamma_{e\text{-}p}$ can be derived from the first principle calculation and γ_e is calculated from conventional SRIM calculation.

2.2 Electron-phonon coupling

Eletron-phonon(e-p) coupling is described by the exchange rate of energy between the electrons and the lattice subsystems [9]. For insulator, behavior of electrons in conduction band can be approximated as free electron gas [11]. Electron-phonon friction coefficient ($\gamma_{e\text{-}p}$) is

$$\gamma_{e-p} = \frac{m}{\tau_{e-p}} \quad (3)$$

where *m* is mass of ion. Electron-phonon relaxation time is predicted by solving Boltzmann transport equation [13-20] with using lowest-order variational approximation (LOVA). Electron-phonon relaxation time ($\tau_{e\text{-}p}$) is given by

$$\frac{1}{\tau_{e-p}} = \frac{4\pi k_B T_p}{\hbar} \int_0^\infty d\omega \frac{\alpha^2 F(\omega)}{\omega} I(\omega/2k_B T_l), \quad (4)$$

where k_B is Boltzmann constant, $\hbar$ is Plank constant, ω is phonon frequency, $\alpha^2F(\omega)$ is Eliashberg spectral distribution function [16-18]. and $I(x) = [x/\sinh(x)]^2$.

We evaluate Eliashberg spectral distribution function ($\alpha^2F(\omega)$) of UO_2 calculated from total energy frozen-phonon approach using supercells [16,17-19] with LDA formalism in ELK codes [22] as in Fig.2.

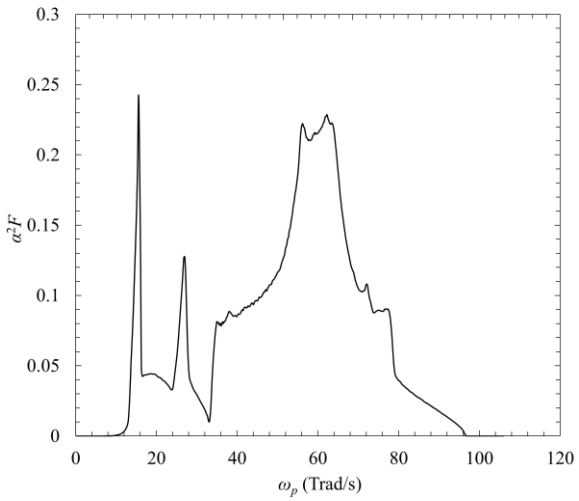

Fig. 1. Eliashberg spectral distribution function as function of phonon frequency.

From the obtained Eliash berg spectral function, e-p relaxation time is evauluated using Eq.(4). And friction coefficient is derived.

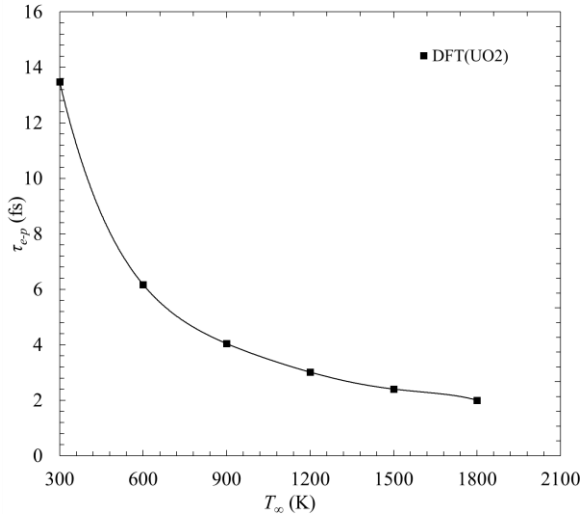

Fig. 2. Variations of the DFT predicted electron-phonon relaxation time as a function of temperature

2.2 Electronic stopping

Electronic stopping friction coefficient (γe) in TTM-MD is determined from electronic stopping. Stopping powers of Cs-137 (HFF) and Sr-90 (LFF) in UO2

matrix are obtained from SRIM calculation in Fig. 3.

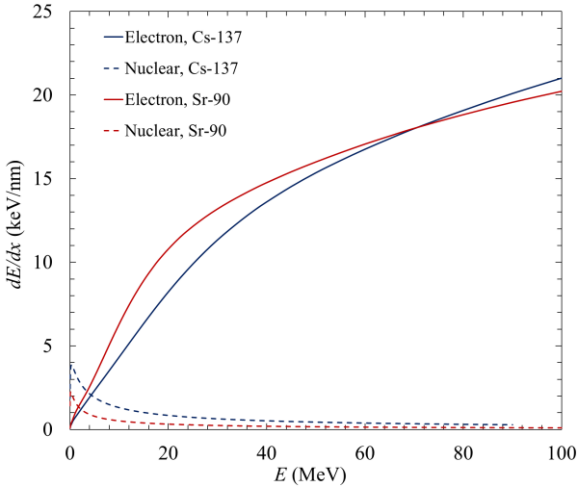

Fig. 3. Stopping power of Cs-137 (red) and Sr-90 (blue) calculated from SRIM calculation. Both electronic (solid lines) and nuclear stopping (broken lines) powers are obtained.

Based on Lindhard and Scharff model [24], electronic stopping power is fitted to square root of kinetic energy of particle:

$$\frac{dE}{dx} = \lambda E^{1/2}, \quad (5)$$

where λ is the constant of proportionality. With the kinetic energy expression of ion, it is converted to

$$m\frac{dv}{dt} = \lambda\left(\frac{m}{2}\right)^{1/2} v. \quad (6)$$

In the analogy with the friction term in Lagevin equation of motion (second term of right hand side in Eq.(2)), electronic stopping friction coefficient (γ_s) is

$$\gamma_e = \lambda\left(\frac{m}{2}\right)^{1/2}. \quad (7)$$

From the SRIM calculations, γ_e is shown to be 0.014 g/mol-ps for Cs-137 and 0.015 g/mol-ps for Sr-90.

2.7 TTM-MD

From obtained parameters from the first principle calculation and SRIM calculation, TTM-MD simulation has been conducted. Electronic heat capacity is assumed to be 10^6 J/m^3-K and electronic thermal conductivity is 20 W/m-K as the approximation of free electron gas in noble metal.

Fission heat deposition by fission fragment is described by delta-ray energy injection term in Eq.(1), rather than primary knock-on atom (PKA) in usual cascade simulations. Energetic particle having order of MeV kinetic energy penetrate the system of MD simulation in atto-second time scale. Since this atto-second time scale cannot be detected in the MD simulation, suppose that delta-ray is already created by penetration of radiative particle, we set initial electronic temperature profile as input parameters. The morphology of electronic temperature can be approximated by a Gaussian distribution in radial direction with cylindrical symmetry. Raising temperature (ΔT_e) is [25]

$$\Delta T = \frac{gS_e}{\rho_e c_e \pi\lambda^2}\exp\left[-\frac{r^2}{\lambda^2}\right], \quad (8)$$

where gS_e is the fraction of energy deposited as stopping power, c_e, ρ_e are electronic specific heat and number density, respectively. The constant (λ) is dependent on the energy (MeV/amu) of the swift ion and may be estimated to be between 1-4 run in UO_2.

We have tested that fission heat is deposited by Cs-137 fission fragment on UO_2 matrix. Stopping power is set to 10 keV/nm. With the initial setting of electronic temperature equivalent to heat deposition by Cs-137, We got the radiation damage picture in Fig. 4. Center part of the solid system is liquidized by heat deposition, which is equivalent to the electronic stopping power by fission fragments

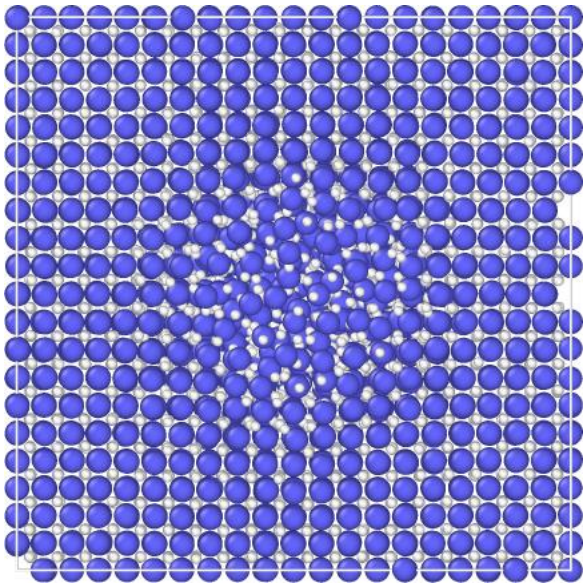

Fig. 4. Snapshot of UO_2 system under the radiation condition. (blue sphere: uranium, white sphere: oxygen)

3. Conclusions

We have investigated the radiation damage effect on material using multi-scale/physics hierarchy. First, electron-phonon coupling parameters for heat diffusion equation between electron-phonon system is evaluated. Second, electronic stopping power is parameterized by SRIM calculation. From parameters from both approaches, TTM-MD framework has been simulated for accurate investigation of radiation effect on materials. Afterward, we have a plan to make the system size

enlarged to describe high stopping range regime and have a comparison with track radius data created by irradiation experiment in same condition with our simulation.

REFERENCES

[1]J.L. Wormald, A.I. Hawari, Examination of the impact of electron–phonon coupling on fission enhanced diffusion in uranium dioxide using classical molecular dynamics, J. Mater. Res. 30 (2015) 1485–1494. doi:10.1557/jmr.2014.405.

[2]V. V Pisarev, S. V Starikov, Atomistic simulation of ion track formation in UO2., J. Phys. Condens. Matter. 26 (2014) 475401. doi:10.1088/0953-8984/26/47/475401.

[3]D.A. Young, Etching of radiation damage in lithium fluoride., Nature. 182 (1958) 375.

[4]J.F. Ziegler, J.P. Biersack, The stopping and range of ions in matter, in: Treatise Heavy-Ion Sci., Springer, 1985: pp. 93–129.

[5].M. Duffy, a M. Rutherford, Including the effects of electronic stopping and electron–ion interactions in radiation damage simulations, J. Phys. Condens. Matter. 19 (2007) 16207. doi:10.1088/0953-8984/19/1/016207.

[6]A. Rutherford, D. Duffy, The effect of electron-ion interactions on radiation damage simulations, 19 (2007) 1–9. doi:10.1088/0953-8984/19/49/496201.

[7]A. Rutherford, D. Duffy, The effect of electron-ion interactions on radiation damage simulations, J. Phys. Condens. Matter. 19 (2007) 1–9. doi:10.1088/0953-8984/19/49/496201.

[8]A.I. Hawari, A. Ougouag, Microscale Heat Conduction Models and Doppler Feedback, North Carolina State Univ., 2015.

[9]D.M. Duffy, N. Itoh, a M. Rutherford, a M. Stoneham, Making tracks in metals, J. Phys. Condens. Matter. 20 (2008) 82201. doi:10.1088/0953-8984/20/8/082201.

[10]Z. Lin, L. V. Zhigilei, V. Celli, Electron-phonon coupling and electron heat capacity of metals under conditions of strong electron-phonon nonequilibrium, Phys. Rev. B - Condens. Matter Mater. Phys. 77 (2008) 1–17. doi:10.1103/PhysRevB.77.075133.

[11]A.I.H. Jonathan L. Wormald, Molecular Dynamics Simulation of the Impact of Fission Fragment Energy Deposition on Ion, Mater. Res. Soc. Symp. Proc. 1771 (2015) 0–5. doi:10.1557/opl.2015.

[12]I.A. Baranov, Y. V Martynenko, S.O. Tsepelevich, Y.N. Yavlinskiĭ, Inelastic sputtering of solids by ions, Sov. Phys. Uspekhi. 31 (1988) 1015.

[13] M. Toulemonde, C. Dufour, A. Meftah, E. Paumier, Transient thermal processes in heavy ion irradiation of crystalline inorganic insulators, Nucl. Instruments Methods Phys. Res. Sect. B Beam Interact. with Mater. Atoms. 166 (2000) 903–912. doi:10.1016/S0168-583X(99)00799-5.

[14]P.B. Allen, Electron-phonon effects in the infrared properties of metals, Phys. Rev. B. 3 (1971) 305–320. doi:10.1103/PhysRevB.3.305.

[15]P.B. Allen, New method for solving Boltzmann's equation for electrons in metals, Phys. Rev. B. 17 (1978) 3725–3734. doi:10.1103/PhysRevB.17.3725.

[16]J.H. Kim, K. Levin, R. Wentzcovitch, A. Auerbach, Electron-phonon interactions in the copper oxides: Implications for the resistivity, Phys. Rev. B. 40 (1989) 11378–11381. doi:10.1103/PhysRevB.40.11378.

[17]D.Y. Savrasov, D.Y. Savrasov, S.Y. Savrasov, S.Y. Savrasov, Electron-phonon interactions and related physical properties of metals from linear-response theory, Phys. Rev. B. 54 (1996) 16487. doi:10.1103/PhysRevB.54.16487.

[18]P.B. Allen, Theory of thermal relaxation of electrons in metals, Phys. Rev. Lett. 59 (1987) 1460–1463. doi:10.1103/PhysRevLett.59.1460.

[19]P.B. Allen, Neutron spectroscopy of superconductors, Phys. Rev. B. 6 (1972) 2577–2579. doi:10.1103/PhysRevB.6.2577.

[20]M.M. Dacorogna, M.L. Cohen, P.K. Lam, Self-Consistent Calculation of the q Dependence of the Electron-Phonon Coupling in Aluminum, Phys. Rev. Lett. 55 (1985) 837–840. doi:10.1103/PhysRevLett.55.837.

[21]A.I. Liechtenstein, I.I. Mazin, C.O. Rodriguez, O. Jepsen, O.K. Andersen, M. Methfessel, Structural phase diagram and electron-phonon interaction in Ba 1− x K x BiO 3, Phys. Rev. B. 44 (1991) 5388.

[22]http://elk.sourceforge.net.

[23]J.L. Wormald, A.I. Hawari, Exploring fission enhanced diffusion of uranium in uranium dioxide using classical molecular dynamics simulations, in: TMS 2014 143rd Annu. Meet. Exhib. Annu. Meet. Suppl. Proc., John Wiley & Sons, 2014: p. 155.

[24]T. Wiss, H. Matzke, C. Trautmann, M. Toulemonde, S. Klaumünzer, Radiation damage in UO2 by swift heavy ions, Nucl. Instruments Methods Phys. Res. Sect. B Beam Interact. with Mater. Atoms. 122 (1997) 583–588. doi:http://dx.doi.org/10.1016/S0168-583X(96)00754-9.

[25] G. Szenes, General features of latent track formation in magnetic insulators irradiated with swift heavy ions, Phys. Rev. B. 51 (1995) 8026–8029. doi:10.1103/PhysRevB.51.8026.